International Journal of Pharmaceutics 425 (2012) 29–34

Contents lists available at SciVerse ScienceDirect

International Journal of Pharmaceutics

journal homepage: www.elsevier.com/locate/ijpharm

Montmorillonite intercalated with glutathione for antioxidant delivery: Synthesis, characterization, and bioavailability evaluation

Miri Baek[a], Jin-Ho Choy[b,*], Soo-Jin Choi[a,**]

[a] Department of Food Science and Technology, Seoul Women's University, Seoul 139-774, Republic of Korea
[b] Center for Intelligent Nano-Bio Materials, Department of Chemistry and Nano Science, Department of Bioinspired Science, Ewha Womans University, Seoul 120-750, Republic of Korea

ARTICLE INFO

Article history:
Received 2 November 2011
Received in revised form
12 December 2011
Accepted 7 January 2012
Available online 14 January 2012

Keywords:
Glutathione
Montmorillonite
Antioxidant activity
Pharmacokinetics
Tissue distribution

ABSTRACT

A most powerful antioxidant, glutathione (GSH), plays an important role in detoxification, immune response, and protection against reactive oxygen species. However, orally ingested GSH can be easily degradable to free amino acids by chemical and enzymatic hydrolysis, resulting in low bioavailability. The aim of this study was, therefore, to enhance GSH bioavailability by developing GSH–montmorillonite (MMT) hybrid system. It was also coated with polyvinylacetal diethylaminoacetate (AEA) for better stability. Both GSH–MMT and AEA–GSH–MMT hybrids were characterized by powder X-ray diffraction (PXRD), Fourier transformed infrared (FT-IR), and thermogravimetric analysis (TGA), indicating that GSH was successfully intercalated into the interlayer spaces of MMT. *In vivo* antioxidant activity assay revealed that AEA–GSH–MMT hybrid significantly increased antioxidant activity in the plasma after oral administration in mice. Pharmacokinetic study also indicated that AEA–GSH–MMT hybrid considerably increased the plasma concentration of GSH at 1 h post-oral administration. Moreover, both the hybrid systems remarkably enhanced GSH delivery to the main target tissue, liver. All the results suggest that GSH–MMT hybrid systems have great potential to enhance bioavailability of oral GSH, providing new insight into their pharmaceutical application.

1. Introduction

Glutathione (γ-L-glutamyl-L-cysteinylglycine,GSH) is a water-soluble tripeptide involved in many biological processes including intermediary metabolism, catalysis, and transport (Bannai and Tateishi, 1986). It also acts as an endogenous antioxidant, playing an important role in the protection of cells against reactive oxygen species by neutralizing free radicals (Brezeninska-Slebodzinska et al., 1995; Milne et al., 1993). Thus, it is known that high concentration of GSH is found in the organs frequently exposed to xenobiotics such as liver, kidney, and intestine (Jewell and O'Brien, 1999). In addition, GSH is essential to maintain the normal function of the immune system as an immune booster, for example, by activating lymphocytes (Li et al., 2007). Therefore, systemic GSH and cysteine depletion have occurred in many diseases such as HIV infection, acute respiratory disease, and Parkinson's disease (Mihm et al., 1991; Jahoor et al., 1999). However, orally ingested GSH can be easily degraded to free amino acids by chemical and enzymatic hydrolysis (Witschi et al., 1992). Oral GSH is hydrolyzed in the intestine by the intestinal gamma-glutamyl transferase, so small amount of GSH reaches the portal circulation from the small intestine during gastrointestinal (GI) transit (Anderson et al., 1980). If any, it is also rapidly metabolized by hepatic gamma-glutamyl transferase, eventually resulting in low absorption rate into the blood circulation and low bioavailability in the tissues (Shaw and Newman, 1979). Moreover, GSH with a thiol group can be easily oxidized both enzymatically and non-enzymatically at alkaline pH such as intestinal environment, giving rise to the formation of glutathione disulphide (GSSG), which is devoid of antioxidant activity (Aw, 2005). In this regard, the development of novel delivery carrier systems can be useful to stabilize and protect labile GSH against harsh biological conditions, subsequently leading to increase its bioavailability following oral ingestion. A few attempts have been made to develop GSH delivery systems, and to the best of our knowledge, no study has clearly demonstrated the efficacy of GSH delivery systems *in vivo* (Aisawa et al., 2006; Trapani et al., 2007).

Montmorillonite (MMT), a natural clay mineral, is a bio-inspired layered material with high internal surface area, high cation exchange capacity (CEC), high adsorption ability, and low toxicity (Lee and Fu, 2003; Komine, 2004). MMT with net negatively charge layers has good swelling property in the presence of water, and therefore, the positively charged bioactive compounds can be intercalated into the interlayer spaces by electrostatic interaction

* Corresponding author. Tel.: +82 2 3277 4135; fax: +82 2 3277 4340.
** Corresponding author. Tel.: +82 2 970 5634; fax: +82 2 970 5977.
E-mail addresses: jhchoy@ewha.ac.kr (J.-H. Choy), sjchoi@swu.ac.kr (S.-J. Choi).

0378-5173/$ – see front matter © 2012 Elsevier B.V. All rights reserved.
doi:10.1016/j.ijpharm.2012.01.015

under this condition (Fudala et al., 1999). Many attempts have been made to develop MMT as a delivery carrier, for example, to improve water solubility of insoluble drugs and release control of bioactive molecules (Zheng et al., 2007; Fudala et al., 1999; Kollár et al., 2003; Lin et al., 2002; Park et al., 2004, 2008). MMT itself has also attractive properties for oral application; it is highly mucoadhesive, which is a useful property for molecules to across the GI barrier (Dobrozsi, 2003). MMT also plays a role as a potent detoxifier in the intestine, since it can adsorb dietary, bacterial, and metabolic toxins as well as abnormally increased hydrogen ions observed in acidosis (Sun et al., 2008). In addition, it is worth noting here that MMT is generally recognized as a low toxic material (Lee et al., 2005), since it is commonly applied in pharmaceutical products as both the excipient and active substance (Wang et al., 2008).

In this work, we attempted to develop GSH–MMT hybrid system by intercalating GSH into the interlayer spaces of MMT. Polymer coating of the hybrid was further processed with polyvinylacetal diethylaminoacetate (AEA) for better stability *in vivo* by oral administration. Chemical characterization was then performed to ensure successful intercalation of GSH into MMT layers. The antioxidant activity of GSH–MMT hybrids with or without AEA coating was investigated *in vivo*, followed by pharmacokinetic and tissue distribution studies in mice after oral administration.

2. Materials and methods

2.1. Materials

Na^+-MMT with a CEC of 0.7–1.1 mequiv./g and AEA were supplied by Sigma–Aldrich (USA) and Sankyo (Japan), respectively. GSH and all the other reagents of high purity were purchased from Sigma–Aldrich (USA).

2.2. Preparation of GSH–MMT hybrids

GSH–MMT hybrid was prepared as follow; first, 10 g of Na^+-MMT was dispersed in 900 ml of de-ionized water and vigorously stirred for 4 h at room temperature. An excess molar ratio of GSH compared with MMT (1.8 fold of CEC) was dissolved in 100 ml of de-ionized water (pH value adjusted to 2.0 with HCl) and added to MMT solution. The final pH of the GSH and MMT mixture solution was adjusted to 2.0 by addition of HCl solution. Thus prepared suspension was stirred at room temperature overnight and finally the resulting product was freeze-dried. To obtain polymer coated GSH–MMT hybrid, the prepared GSH–MMT hybrid was redispersed in 800 ml of ethanol solution, and 10 g of AEA in 100 ml of methylene chloride (MC) was then added. The final AEA–GSH–MMT hybrid was spray dried (EYLA spray dryer SD-1000, Tokyo, Japan) under the following condition: atomizing pressure, 130 kPa; blower speed, 0.30 m^3/min; inlet temperature, 80 °C; and outlet temperature 40–50 °C.

2.3. Characterization of GSH–MMT hybrids

The prepared GSH–MMT hybrids were characterized by powder X-ray diffraction (PXRD) using a diffractometer (Rigaku D/MAX RINT 2200-Ultima+, Japan) with Ni-filtered CuKα radiation (λ = 1.5418 Å, voltage of 40 kV, a current of 30 mA, and a scanning rate of 2°/min) and Fourier transform infrared (FT-IR) spectroscopy (JASCO FT-IR-6100 spectrometer, Tokyo, Japan) analyses using the standard KBr disk method, respectively. Thermogravimetric analysis (TGA) was performed on a PerkinElmer instrument (pyris diamond TG-DTA, Japan) using a heating rate of 20 °C/min up to 800 °C in nitrogen atmosphere.

2.4. Determination of GSH content

GSH intercalation efficiency into MMT layers was analyzed by dispersing 100 mg of GSH–MMT hybrid or AEA–GSH–MMT hybrid in 100 ml solution consisting of 50 mM $NaClO_4$ 0.1% H_3PO_4. The mixture solution was vigorously vortexed and sonicated for 40 min to completely extract all the GSH from the MMT lattice. The suspension was then filtered by a nylon membrane with a pore size of 0.45 μm (Whatman, UK) and GSH content was then measured by high performance liquid chromatography (HPLC) using an LC10-ADVP series (Shimadzu Co., Japan) on a Discovery RP-Amide 16 column (150 mm × 4.6 mm, 5 μm; Sigma, USA). The mobile phase was 50 mM $NaClO_4$ 0.1% H_3PO_4 and flow rate was set to 1 ml/min. Column temperature was maintained at 40 °C and detection of GSH was performed at 215 nm by UV detector (Yilmaz et al., 2009).

2.5. Animal and diets

Male ICR mice, aged 5.5 weeks and weighing 23–25 g, were purchased from the G-Bio (South Korea). The animals were housed in plastic lab animal cages in a ventilated room. The room was maintained at 20 ± 2 °C and 60 ± 10% relative humidity with a 12 h light/dark cycle. Water and commercial laboratory complete food for mice were available *ad libitum*. They were acclimated to this environment for 7 days before treatment. All animal experiments were performed in compliance with the Animal and Ethnics Review Committee of the Seoul Women's University.

2.6. Antioxidant activity in vivo

To evaluate *in vivo* antioxidant effect of the hybrids, the blood samples were collected after oral administration of free GSH, GSH–MMT hybrid, or AEA–GSH–MMT hybrid by gavage at several time points (0, 15 min, 30 min, 1 h, 2 h, and 4 h) in each group of five mice. The dose of the hybrids was adjusted to have an equivalent amount of 100 mg/kg of GSH, based on GSH content from the hybrids. The blood samples were centrifuged at 3000 rpm for 15 min at 4 °C, and the plasma was used to assess 2,2′-azinobis-3-ethyl-benzothiozoline-6-sulphonic acid (ABTS) radical scavenging activity as follow; ABTS radicals were produced by mixing 10 mM ABTS and 10 mM potassium persulfate with a volume ratio of 7.4 to 2.6 for the former and the latter, respectively, followed by incubation for 24 h in the dark at 37 °C. Then, ABTS radical solution was diluted in phosphate buffered saline (PBS) and mixed with the sample solution (volume ratio of ABTS radical solution:sample solution = 2:13) until the absorbance reached about 0.9, and further incubated for 30 min in the dark. The absorbance was measured at 734 nm. The five mice administered without GSH or the hybrids were used as a control group.

2.7. Pharmacokinetic study

The plasma concentration of GSH was analyzed after oral administration of GSH or the hybrids in mice. The blood samples (about 0.5 ml) were collected *via* orbital sinus at several time points (0, 15 min, 30 min, 1 h, 2 h, and 4 h). The same doses used for *in vivo* antioxidant activity were administered to each group of five mice. The blood sample at 0 h before oral administration was used to determine the basal GSH level in the plasma. The blood samples were centrifuged at 3000 rpm for 15 min at 4 °C to obtain the plasma and stored at −70 °C before analysis. The proteins in the plasma were precipitated by adding 4 volume of acetonitrile, followed by vortexing for 20 s, and centrifuging at 10,000 rpm for 10 min at 4 °C. GSH concentration in the supernatant was measured by HPLC as described above. Calibration curve for GSH in the plasma was obtained by preparing a series of plasma standard solution

with a concentration of 5, 10, 50 μg/ml. The following pharmacokinetic parameters were estimated using Kinetica program (version 4.4, Thermo Electron Corporation, USA): maximum concentration (C_{max}), time to maximum concentration (T_{max}), area under the plasma concentration-time curve (AUC), half-life ($T_{1/2}$), and mean residence time (MRT).

2.8. Tissue distribution study

To evaluate delivery efficiency of GSH to the organs, the tissue samples such as brain, heart, kidney, liver, lung, and intestine were collected at 0, 1, 2, 4, and 6 h post-oral administration. 100 mg of each tissue were homogenized with the mixture of 3 ml 10 mM EDTA, 50 mM $NaClO_4$, and 0.1% H_3PO_4 buffer, followed by addition of 0.5% metaphosphoric acid for protein precipitation. The samples were vortexed for 20 s, centrifuged at 10,000 rpm at 4 °C, and then analyzed by HPLC as described above. Calibration curve for GSH in the tissues was obtained by preparing a series of tissue standard solution with a concentration of 10, 50, 100 μg/ml.

2.9. Statistical analysis

The data were expressed as means ± standard deviation. For statistical analysis, the experimental values were compared with their corresponding control ones. A one-way analysis of variance (ANOVA) in SAS software (Turkey's Test, Version 11.0) was used to illustrate the significant difference between the experimental group and the control. The statistical significance for all tests was set at $p < 0.05$.

3. Results and discussion

3.1. PXRD analysis

We have synthesized GSH–MMT hybrid system by intercalating GSH into the negatively charged Na-MMT layers at pH 2.0 where cation exchange reaction occurred between sodium ions and protonated GSH. A part of thus prepared hybrid was further coated with cationic gastric soluble polymer, AEA, widely used in tablets or microcapsules to obtain better stability and dispersity (Choy et al., 2008). Fig. 1 showed the PXRD pattern of MMT and GSH–MMT hybrid. The characteristic 2θ peaks for MMT and GSH–MMT hybrid were found at 7.40° and 4.34° and the d-spacing for the former and the latter were calculated to be 12.54 Å and 20.43 Å, respectively, upon molecular size of interlayer GSH according to the Bragg's law.

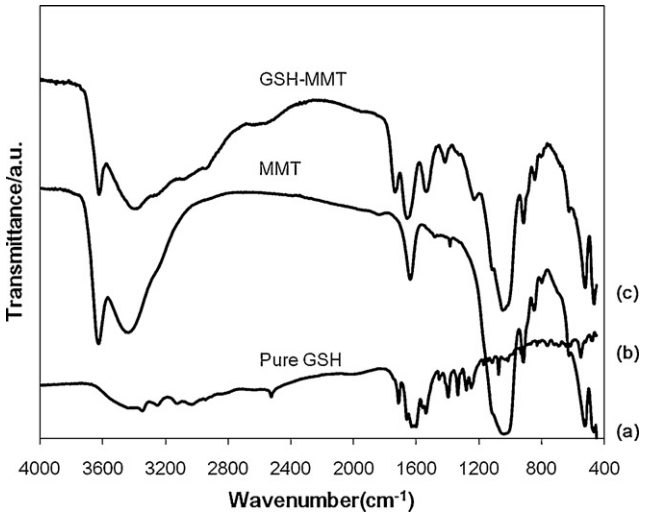

Fig. 2. FT-IR spectra of (a) MMT, (b) pure GSH, and (c) GSH–MMT hybrid.

The peak shifting from higher diffraction angle to lower one is resulted from increased the d-spacing, indicating successful interaction of GSH into the interlayer spaces of MMT. The diagrams of expected GSH–MMT hybrid was also presented (Fig. 1), representing GSH structure in a monomer form after intercalation into MMT layers on the basis of XRD pattern. This result suggests that GSH could be intercalated into MMT layers without inducing glutathione disulphide during synthetic process, which is critical for antioxidant activity.

3.2. FT-IR spectra analysis

FT-IR spectra of MMT, pure GSH, and GSH–MMT hybrid were recorded in Fig. 2. The spectrum of MMT showed the characteristic absorption bands at 3400 and 3620 cm^{-1} which correspond to —OH stretching band for absorbed interlayer water and —OH band stretch for Al—OH, respectively. The absorption peak at 1640 cm^{-1} is attributed to —OH bending mode of the absorbed water. The characteristic peak at 1150 and 1035 cm^{-1} are due to Si—O stretching (out-of-plane) for MMT and Si—O stretching (in-plane) vibration for layered silicates, respectively. The peaks at 915, 875, and 836 cm^{-1} are attributed to Al—Al—OH, Al—Fe—OH, and Al—Mg—OH bending vibrations, respectively (Patel et al., 2007). In the case of pure GSH, the strong absorption bands at 1713 and 1600 cm^{-1} are

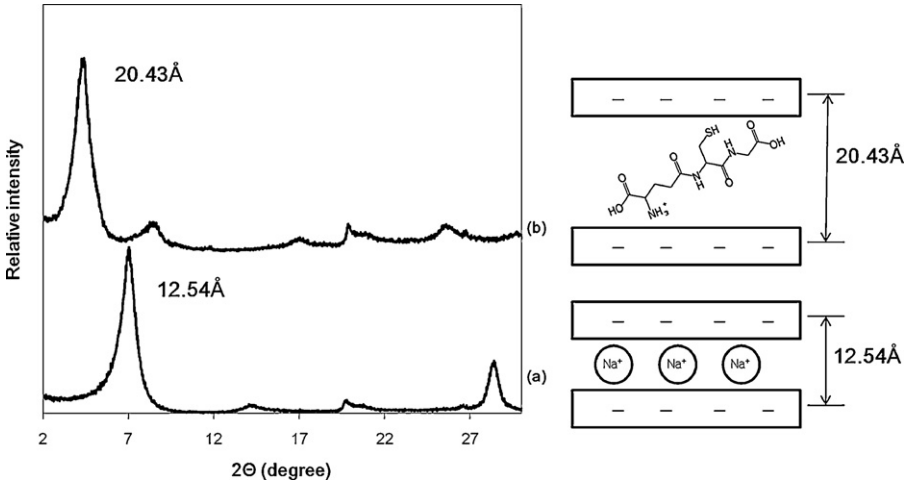

Fig. 1. PXRD patterns and schematic diagram of (a) MMT and (b) GSH–MMT hybrid.

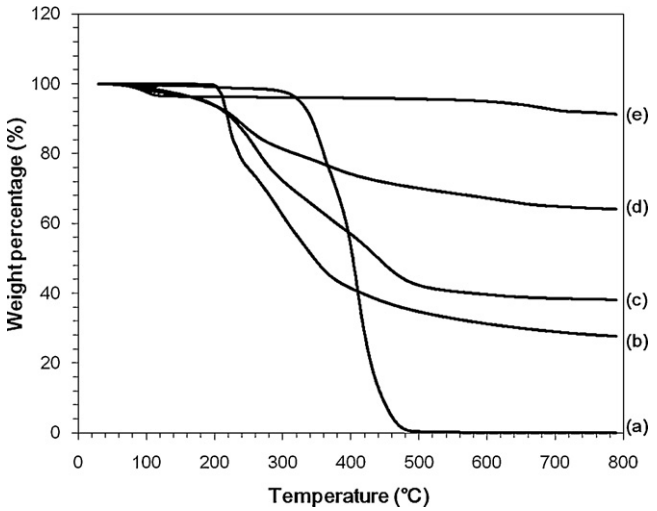

Fig. 3. TGA curves of (a) AEA, (b) pure GSH, (c) AEA–GSH–MMT hybrid, (d) GSH–MMT hybrid, and (e) MMT.

assigned to carbonyl- and amide-stretching, respectively, and the absorption band of sulfhydryl group from cysteine appeared at 2525 cm^{-1}. FT-IR spectrum of GSH–MMT hybrid showed a continuum observed beginning at about 2800 cm^{-1} and extended toward lower wavenumber at about 1800 cm^{-1}, which seems to be resulted from the formation of hydrogen bonds between GSH and MMT (Brzezinski et al., 1995). In the case of GSH–MMT hybrid, the strong absorption band at 1713 cm^{-1} corresponding to carbonyl-stretching of pure GSH was not disappeared, indicating that GSH was well intercalated into MMT layers.

3.3. Thermal analysis

Fig. 3 depicts the TGA curves of pure GSH, MMT, AEA, GSH–MMT hybrid, and AEA–GSH–MMT hybrid. The TGA curves of MMT represent two distinct steps. The first major weight loss pattern observed at the temperature of below 150 °C is due to the free water evaporation. The second step of decomposition at 600–750 °C corresponds to the loss of structural hydroxyl group (Magaraphan et al., 2001). Meanwhile, pure GSH shows a sharp weight loss at around 200–400 °C, indicating strong endothermic peak at this temperature. In the case of GSH–MMT and AEA–GSH–MMT hybrids, the TGA curves are divided into three steps: the weight loss at 200–500 °C is due to decomposition of GSH absorbed on MMT and other weight losses are the same as observed in the TGA curve of MMT. High decomposition rate of AEA–GSH–MMT hybrid was observed compared with GSH–MMT hybrid, which is highly related to a sharp weight loss of AEA at around 300–500 °C. According to the TGA curves, pure GSH exhibited a 72.35% weight loss, while the weight loss of MMT was only 8.75% in the range of the same temperature. It is, therefore, concluded that the weight loss of GSH–MMT hybrid (35.94%) and AEA–GSH–MMT hybrid (61.89%) can be rationally attributed to free GSH intercalated into MMT layers. All the results on the characterization of GSH–MMT hybrids confirmed successful interaction of GSH into MMT.

3.4. GSH content analysis

To improve bioavailability of GSH through GSH–MMT hybrid systems, it is indispensable that large amount of GSH is intercalated into the interlayer spaces of MMT. The result demonstrated that GSH–MMT hybrid and AEA–GSH–MMT hybrid had 38.57 ± 2.22% and 24.09 ± 0.70% of GSH contents, respectively. It seems that GSH content from AEA–GSH–MMT hybrid was reduced by re-dispersing GSH–MMT hybrid in ethanol-MC mixture solution during the coating process, but both GSH–MMT and AEA–GSH–MMT hybrids were determined to have sufficient GSH content to apply at the systemic level.

3.5. Antioxidant activity in vivo

Table 1 represents the antioxidant effect of GSH–MMT hybrids, measured by ABTS radical scavenging assay in the plasma after oral administration in mice. When free GSH or GSH–MMT hybrid was orally administered, significant increase in ABTS radical scavenging activity was not found compared with control group. However, AEA–GSH–MMT hybrid significantly enhanced the antioxidant activity in the plasma at 1 h post-oral administration, suggesting increased bioavailability of GSH through the AEA-coated hybrid system *in vivo*. Both AEA polymer alone and MMT itself did not have ABTS radical scavenging activity (data not shown). It is likely that the high radical scavenging activity of AEA–GSH–MMT hybrid is closely associated with further stabilization process, AEA coating.

3.6. Pharmacokinetics

Pharmacokinetic study was conducted to determine the pharmacokinetic parameters of the hybrids, which can provide direct information to evaluate whether the hybrid system can enhance the bioavailability of GSH or not. The data were presented after subtraction of basal GSH level in the plasma (Fig. 4). The result demonstrated that C_{max} of GSH was found at 30 min after administration of free GSH, which is well consistent with a rapid absorption of GSH from the intestinal lumen to the plasma (Hagen et al., 1990). No significant difference in the plasma concentration profile was seen between free GSH and GSH–MMT hybrid-treated groups. On the other hand, the peak concentration significantly increased about 2.9 fold at 1 h post-oral administration in comparison with that of free GSH or GSH–MMT hybrid when AEA–GSH–MMT hybrid was administered in mice (Fig. 4). This result suggests that high amount of GSH could reach the circulation system through AEA–GSH–MMT hybrid system, probably by protecting GSH against harsh biological conditions such as enzyme attack and low pH.

The pharmacokinetic parameters were also presented in Table 2. All the parameters of AEA–GSH–MMT hybrid showed considerably high values compared with those of free GSH. Especially, AUC of AEA–GSH–MMT hybrid increased about 4.7 fold in comparison with that of free GSH. AUC represents the total amount of a

Table 1
In vivo antioxidant activity of free GSH, GSH–MMT hybrid, and AEA–GSH–MMT hybrid in the plasma after oral administration in mice, measured by ABTS radical scavenging activity.

Treated group	ABTS radical scavenging activity (%)					
	Control	0.25 h	0.5 h	1 h	2 h	4 h
GSH	57.42 ± 2.00	53.73 ± 4.35	53.86 ± 5.09	57.34 ± 6.67	57.31 ± 2.38	58.21 ± 2.32
GSH–MMT	57.42 ± 2.00	58.77 ± 5.09	53.90 ± 4.84	52.80 ± 2.83	53.83 ± 1.02	57.02 ± 4.01
AEA–GSH–MMT	57.42 ± 2.00	60.77 ± 4.22	60.12 ± 1.02	61.97 ± 2.05*	52.77 ± 4.16	59.88 ± 2.98

* Significant difference from the control ($p < 0.05$).

Table 2
Pharmacokinetic parameters of free GSH, GSH–MMT hybrid, and AEA–GSH–MMT hybrid after oral administration in mice.

	C_{max} (mg/l)	T_{max} (h)	AUC (h × mg/l)	$T_{1/2}$ (h)	MRT (h)
GSH	29.51	0.50	21.01	0.73	1.33
GSH–MMT	34.22	0.50	44.34	0.97	1.58
AEA–GSH–MMT	85.86	1.00	99.18	1.02	1.94

drug or bioactive molecule that reaches the blood circulatory system in a given time, and can be used as a measure how much it stays at the systemic level. The highest C_{max} and AUC values were obtained by AEA–GSH–MMT hybrid, which can also explain its increased antioxidant activity *in vivo* (Table 1). Moreover, T_{max} values of AEA–GSH–MMT hybrid were delayed at 1 h compared with those of free GSH or GSH–MMT hybrid at 30 min, which is well consistent with the enhanced ABTS radical scavenging activity at 1 h *in vivo* (Table 1), probably related to their structural stability and controlled release property. About 1.4–1.5 fold increased $T_{1/2}$ and MRT values of AEA–GSH–MMT hybrid, representing half-life and mean residence time in the body, respectively, suggest that the hybrid could also prolong the circulation time of GSH. Thus, this is clear evidence that the hybrid system effectively enhanced bioavailability of GSH *in vivo*, by not only increasing the systemic circulation amount of GSH, but also prolonging its circulation time. It should be also noted that all the parameters of GSH–MMT hybrid except T_{max} values slightly increased. It seems that AEA–GSH–MMT hybrid is more effective than GSH–MMT hybrid in terms of antioxidant activity *in vivo* and pharmacokinetic behaviors, which is likely to be attributed to its high structural stability resulted from AEA coating.

3.7. Tissue distribution

Several tissues such as brain, heart, kidney, liver, lung, and intestine were also collected after oral administration of the hybrids in mice to evaluate bio-distribution and delivery efficiency to the organs. Interestingly, GSH content in the liver significantly increased by oral administration of both GSH–MMT and AEA–GSH–MMT hybrids in mice (Fig. 5). In the case of GSH–MMT hybrid, delivery efficiency of GSH significantly enhanced at 1 h post-oral administration, although its pharmacokinetics were not significantly different from those of free GSH as shown in Fig. 4. This result suggests that the hybrid system itself without polymer coating could be also effective in terms of GSH delivery to the liver, probably related to the protection role of MMT carrier in enzyme hydrolysis. On the other hand, high delivery

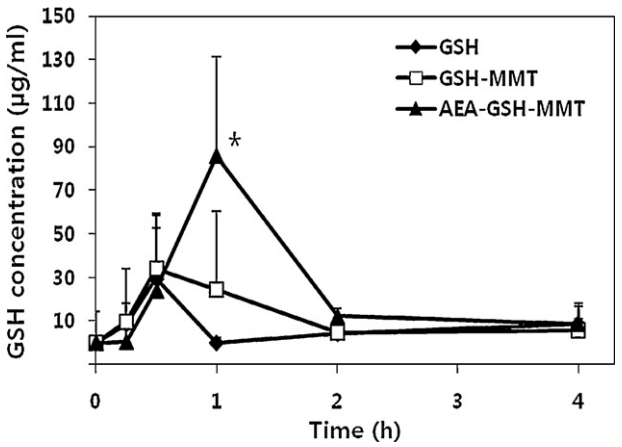

Fig. 4. Plasma concentration of GSH after oral administration of free GSH, GSH–MMT hybrid, or AEA–GSH–MMT hybrid in mice. * denotes a significant difference from the control ($p < 0.05$).

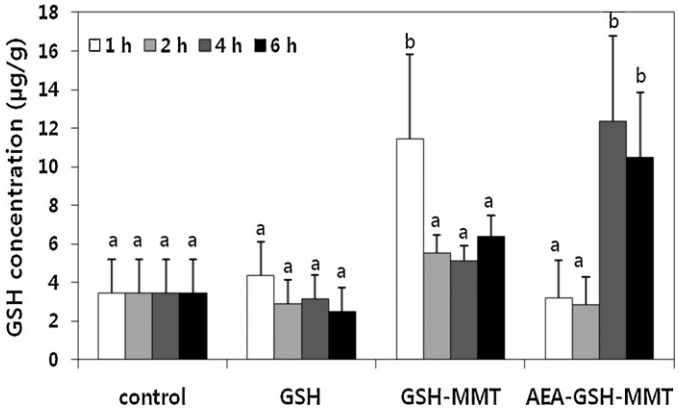

Fig. 5. GSH concentration in the liver after oral administration of free GSH, GSH–MMT hybrid, and AEA–GSH–MMT hybrid in mice. [b] represents a significant increase from the control level indicated as [a] ($p < 0.05$).

efficiency of AEA–GSH–MMT hybrid to the liver was evident at 4–6 h post-administration. The difference between two hybrid systems can be explained by a better controlled release property of the AEA–GSH–MMT at the systemic level due to AEA coating. This result clearly suggests that AEA coating highly contributes to deliver GSH to the liver in a controlled manner by further stabilizing and protecting GSH against biological conditions. Meanwhile, significant increase in GSH concentration was found in the intestine at 1–4 h after administration of free GSH and the hybrids, but remarkable difference between them was not found (data not shown). Increased GSH level was not detected in the other organs (data not shown). To the best of our knowledge, no research has clearly demonstrated the delivery efficiency of GSH with or without delivery systems to the liver in normal mice. It was only reported that orally administered free GSH increased GSH level in several tissues such as kidney, heart, lung, brain, small intestine, and skin, but not in the liver, in GSH-deficient model mice pre-treated with a GSH synthesis inhibitor for 5 days (Aw et al., 1991). In the present study, it is worthy to note here that GSH level significantly increased in the liver, a main target organ where GSH plays a critical role in many biological processes, by using two different hybrid systems, even in normal mice under GSH-sufficient condition. This result strongly implies GSH delivery efficiency through both the hybrid systems.

4. Conclusion

In this study, we have successfully intercalated a powerful antioxidant GSH into the interlayer spaces of MMT and two different hybrid systems, GSH–MMT and AEA–GSH–MMT, were obtained, respectively. AEA–GSH–MMT hybrid system had not only enhanced antioxidant activity *in vivo*, but also favorable pharmacokinetic behaviors such as increased systemic circulation amount and prolonged circulation time of GSH. Delivery efficiency of GSH to the organ was clearly demonstrated by high GSH level in the liver, a main target organ, after oral administration of both the hybrid systems in mice. AEA–GSH–MMT was more effective in terms of antioxidant activity *in vivo*, pharmacokinetics, and delivery efficiency in a controlled manner. Therefore, all the results suggest that GSH–MMT hybrid systems have great potential to

enhance bioavailability of oral GSH, providing new insight into their pharmaceutical application.

Acknowledgments

This work was supported by Basic Science Research Program through the National Research Foundation of Korea (NRF) funded by the Ministry of Education, Science and Technology (2011-0003755), and partly by National Research Foundation of Korea (NRF) Grant funded by the Korean Government (MEST) (SRC Program: 2011-0001340) and by the Ewha Global Top 5 Grant 2011 of Ewha Womans University.

References

Aisawa, S., Sasaki, S., Takahashi, S., Hirahara, H., Nakayama, H., Narita, E., 2006. Intercalation of amino acids and oligopeptides into Zn–Al layered double hydroxide by coprecipitation reaction. J. Phys. Chem. Solids 67, 920–925.

Anderson, M.E., Bridges, R.J., Meister, A., 1980. Direct evidence for inter-organ transport of glutathione and that the non-filtration renal mechanism for glutathione utilization involves (-glutamyl transpeptidase. Biochem. Biophys. Res. Commun. 96, 848–853.

Aw, T.Y., 2005. Intestinal glutathione: determinant of mucosal peroxide transport, metabolism, and oxidative susceptibility. Toxicol. Appl. Pharmacol. 204, 320–328.

Aw, T.Y., Wierzbicka, G., Jones, D.P., 1991. Oral glutathione increases tissue glutathione in vivo. Chem. Biol. Interact. 80, 89–97.

Bannai, S., Tateishi, N., 1986. Role of membrane transport in metabolism and function of glutathione in mammals. J. Membr. Biol. 89, 1–8.

Brezeninska-Slebodzinska, E., Slebodzinski, A.B., Pietras, B., Wieczorek, G., 1995. Antioxidant effect of vitamin E and glutathione on lipid peroxidation in boar semen plasma. Biol. Trace Elem. Res. 47, 69–74.

Brzezinski, B., Labowski, M., Zundel, G., 1995. Disulphide bond formation by glutathione via the glutathione-trimethylamine-N-oxide complex. J. Mol. Struct. 354, 127–130.

Choy, J.H., Park, T., Lee, Y.J., Kim, D.Y., Park, J.K., 2008. Base forming drug-layered silicate hybrid containing basic polymer and its synthesis method. US Patent Appl. US 2008/0119519 A1.

Dobrozsi, D., 2003. Oral liquid mucoadhesive compositions. US Patent US 6,638,521 B2.

Fudala, A.A., Palinko, I.I., Kiricsi, I., 1999. Preparation and characterization of hybrid organic-inorganic composite materials using the amphoteric property of amino acids: amino acid intercalated layered double hydroxide and montmorillonite. Inorg. Chem. 38, 4653–4658.

Hagen, T.M., Wierzbicka, G.T., Bowman, B.B., Aw, T.Y., Jones, D.P., 1990. Fate of dietary glutathione: disposition in the gastrointestinal tract. Am. J. Physiol. Gastrointest. Liver Physiol. 259, G530–G535.

Jahoor, F., Jackson, A., Gazzard, B., Philips, G., Sharpstone, D., Frazer, M.E., Heird, W., 1999. Erythrocyte glutathione deficiency in symptom-free HIV infection is associated with decreased synthesis rate. Am. J. Physiol. Endocrinol. Metab. 276, E205–E211.

Jewell, C., O'Brien, N.M., 1999. Effect of dietary supplementation with carotenoids on xenobiotic metabolizing enzymes in the liver, lung, kidney and small intestine of the rat. Br. J. Nutr. 81, 235–242.

Kollár, T., Pálinko, I., Kónya, Z., Kiricsi, I., 2003. Intercalating amino acid guests into montmorillonite host. J. Mol. Struct. 651–653, 335–340.

Komine, H., 2004. Simplified evaluation for swelling characteristics of bentonites. Eng. Geol. 71, 256–279.

Lee, W.F., Fu, Y.-T., 2003. Effect of montmorillonite on the swelling behavior and drug-release behavior of nanocomposite hydrogels. J. Appl. Polym. Sci. 89, 3652–3660.

Lee, Y.H., Kuo, T.F., Chen, B.Y., Feng, Y.K., Wen, Y.R., Lin, W.C., Lin, F.H., 2005. Toxicity assessment of montmorillonite as a drug carrier for pharmaceutical applications: yeast and rats model. Biomed. Eng. Appl. Basis Commun. 17, 12–18.

Li, P., Yin, Y.L., Li, D., Kim, S.W., Wu, G., 2007. Amino acids and immune function. Br. J. Nutr. 98, 237–252.

Lin, F.H., Lee, Y.H., Jian, C.H., Wong, J.M., Shieh, M.J., Wang, C.Y., 2002. A study of purified montmorillonite intercalated with 5-fluorouracil as drug carrier. Biomaterials 23, 1981–1987.

Magaraphan, R., Lilayuthalert, W., Sirivat, A., Schwank, J.W., 2001. Preparation, structure, properties and thermal behavior of rigid-rod polyimide/montmorillonite nanocomposites. Compos. Sci. Technol. 61, 1253–1264.

Mihm, S., Ennen, J., Pessara, U., Kurth, R., Droge, W., 1991. Inhibition of HIV-1 replication and NF-x B activity by cysteine and cysteine derivatives. AIDS 5, 497–504.

Milne, L., Nicotera, P., Orrenius, S., Burkitt, M.J., 1993. Effects of glutathione and chelating agents on copper-mediated DNA oxidation: pro-oxidant and antioxidant archproperties of glutathione. Arch. Biochem. Biophys. 304, 102–109.

Park, J.K., Choy, Y.B., Oh, J.M., Kim, J.Y., Hwang, S.J., Choy, J.H., 2008. Controlled release of donepezil intercalated in smectite clays. Int. J. Pharm. 359, 198–204.

Park, M., Kim, C.Y., Lee, D.H., Choi, C.L., Choi, J., Lee, S.R., Choy, J.H., 2004. Intercalation of magnesium-urea complex into swelling clay. J. Phys. Chem. Solids 65, 409–412.

Patel, H.A., Somani, R.S., Bajaj, H.C., Jasra, R.V., 2007. Synthesis and characterization of organic bentonite using Gujarat and Rajasthan clays. Curr. Sci. 92, 1004–1009.

Shaw, L.M., Newman, D.A., 1979. Hydrolysis of glutathione by human liver gamma-glutamyltransferase. Clin. Chem. 25, 75–79.

Sun, B., Ranganathan, B., Feng, S.S., 2008. Multifunctional poly(D,L-lactide-co-glycolide)/montmorillonite (PLGA/MMT) nanoparticles decorated by transtuzumab for targeted chemotherapy of breast cancer. Biomaterials 29, 475–486.

Trapani, A., Laquintana, V., Denora, N., Cutriqnelli, A., Franco, M., Tranpani, G., Liso, G., 2007. Eudragit RS 100 microparticles containing 2-hydroxypropyl-beta-cyclodextrin and glutathione: physicochemical characterization, drug release and transport studies. Eur. J. Pharm. Sci. 30, 64–74.

Wang, X., Du1, Y., Luo, J., 2008. Biopolymer/montmorillonite nanocomposite: preparation, drug-controlled release property and cytotoxicity. Nanotechnology 19, 065707.

Witschi, A., Reddy, S., Stofer, B., Lauterburg, B.H., 1992. The systemic availability of oral glutathione. Eur. J. Clin. Pharmacol. 43, 667–669.

Yilmaz, Ö., Keser, S., Tuzcu, M., Güvenc, M., Cetintas, B., Irtegün, S., Tastan, H., Sahin, K., 2009. A practical HPLC method to measure reduced (GSH) and oxidized (GSSG) glutathione concentrations in animal tissues. Int. J. Anim. Vet. Adv. 8, 343–347.

Zheng, J.P., Luan, L., Wang, H.Y., Xi, L.F., Yao, K.D., 2007. Study on ibuprefen/montmorillonite intercalation composites as drug release system. Appl. Clay Sci. 36, 297–301.